

Kinetics of the $\text{HO}_2 + \text{BrO}$ Reaction Over the Temperature Range 233-348 K

Zhuangjie Li¹, Randall R Friedl and Stanley P. Sander*

M/S 183-901, Jet Propulsion Laboratory, California Institute of Technology
Pasadena, California 91109

Abstract

The reaction $\text{BrO} + \text{HO}_2 \rightarrow \text{products}$ is the rate-limiting step in a key catalytic ozone destruction cycle in the lower stratosphere. In this study a discharge flow reactor coupled with molecular beam mass spectrometry has been used to study the $\text{BrO} + \text{HO}_2$ reaction over the temperature range 233-348 K. Rate constants were measured under pseudo-first order conditions in separate experiments with first HO_2 and then BrO in excess in an effort to identify possible complications in the reaction conditions. At 298 K, the rate constant was determined to be $(1.73 \pm 0.61) \times 10^{-12} \text{ cm}^3 \text{ molecule}^{-1} \text{ s}^{-1}$ with HO_2 in excess and $(2.05 \pm 0.64) \times 10^{-12} \text{ cm}^3 \text{ molecule}^{-1} \text{ s}^{-1}$ with BrO in excess. The combined results of the temperature-dependent experiments gave the following fit to the Arrhenius expression: $k = (3.13 \pm 0.33) \times 10^{-12} \exp(536 \pm 206/T)$ where the quoted uncertainties represent two standard deviations. The reaction mechanism is discussed in light of recent *ab initio* results on the thermochemistry of isomers of possible reaction intermediates.

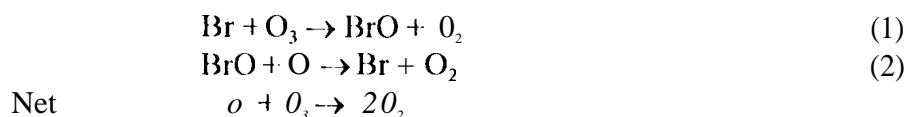
* Corresponding author

Present Address: Department of Atmospheric Sciences, University of Illinois,
Urbana, IL 61801-3070

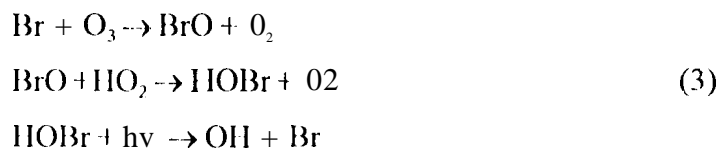
Introduction

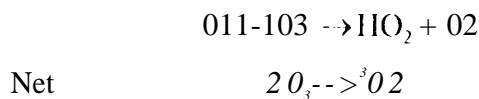
Bromine chemistry plays a key role in the catalytic obstruction of stratospheric ozone. The most important bromine-containing source gas, methyl bromide, has an ozone depletion potential which exceeds the limits set by international treaties, and will be phased out in developed countries by the year **2010**¹. However, because methyl bromide has both biogenic and anthropogenic source fluxes which are highly uncertain, the budgets and atmospheric lifetime of methyl bromide have not been accurately determined. Most other bromine source gases of importance, including the halons, are entirely anthropogenic in origin and their production has ceased in developed countries. Despite the regulatory controls in place however, there are many issues relating to both the gas-phase and heterogeneous chemistry of bromine compounds that require further investigation,

The catalytic cycles that contribute to the destruction of ozone by bromine were first described by Wofsy et al.² and Yung et al.³. By analogy to the well-known O + ClO cycle, Wofsy et al. proposed the cycle

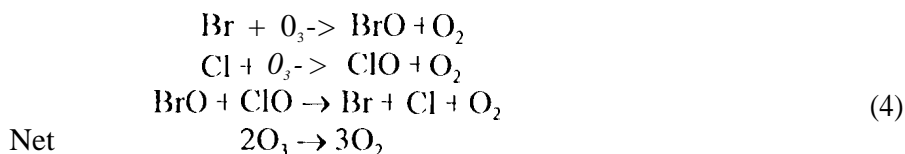


This cycle has its greatest effect on ozone destruction in the middle and upper stratosphere. Yung et al. pointed out several additional cycles that are particularly important in the lower stratosphere that couple bromine radicals with the odd hydrogen and odd chlorine radical families:





and



In these cycles, reactions 3 and 4 are the rate-limiting steps. Reaction 4 has been studied extensively over the temperature and pressure range relevant to the stratosphere and is reasonably well understood^{4,5}. In contrast, significant kinetic and mechanistic uncertainties remain in the understanding of reaction 3.

The first study of reaction 3 was carried out by Cox and Sheppard who reported a rate coefficient of $0.5_{-0.3}^{+0.5} \times 10^{-11} \text{ cm}^3 \text{ molecule}^{-1} \text{ s}^{-1}$ at 303 K and 7150 Torr total pressure using molecular-modulation coupled with ultraviolet absorption⁶. Three recent studies, however, have reported values of k_{298} which were more than 6 times larger than the work of Cox and Sheppard including two discharge flow/mass spectrometry studies from the CNRS group and a flash photolysis/ultraviolet absorption study from the group at Bordeaux⁷⁻⁹. These measurements have a major effect on atmospheric model predictions of bromine partitioning in the lower stratosphere, the relative magnitudes of the odd oxygen destruction cycles involving bromine and the ozone depletion potential of methyl bromide^{1,7}. More recently however, a discharge flow/mass spectrometry study by Elrod et al.¹⁰ reported a significantly smaller value of k_{298} , $(1.4 \pm 0.3) \times 10^{-11} \text{ cm}^3 \text{ molecule}^{-1} \text{ s}^{-1}$.

The large discrepancies between the previously reported results and the importance of this reaction in stratospheric bromine chemistry motivated the study reported here. In this work, the $\text{BrO} + \text{HO}_2$ reaction was investigated over the temperature range 233-348 K using the

discharge flow/mass spectrometry technique. In an effort to identify possible complications in the reaction conditions, rate coefficients were measured using several different BrO and HO₂ sources and separately with BrO and HO₂ as the excess reagent.

Experimental

The experimental apparatus used in these studies has been described previously.^{11,12} Details of the flow reactor and sliding injector are shown in Figure 1. The reactor consisted of a 80 cm-long, 4.86 cm-id. Pyrex tube which was covered on the inside with a layer of 0.05 cm thick TFE Teflon sheet to reduce BrO and HO₂ wall loss. The reactor temperature was varied between 233 and 348 K by circulating cooled methanol or heated ethylene glycol through an outer Pyrex jacket. The temperatures of the circulating fluids were measured with a thermocouple located in the outer jacket of the reactor and controlled to within ± 2 K using a thermostatted heat exchanger. A steady state gas flow (total pressure of 1~3 Torr) was maintained in the flow tube with a 00 cfm mechanical pump (Welch 1396), Helium was used as the main buffer gas and was admitted through sidearm located upstream of the reactor. The mean gas velocity in the flow tube ranged between 800 and 2000 cm s⁻¹; resulting in residence times between 30-75 ms in the 60 cm reaction zone. In order to carry out kinetics measurements at low temperatures, a heated double sliding injector was employed. It consisted of two concentric tubes having i.d.'s of 8 and 10.2 mm, respectively. The movable injector was heated by passing current through heating wire wrapped around the outer injector tube. This tube was thermally isolated from the flow tube with a vacuum jacket. The injector temperature was controlled by varying the voltage applied to the heating wire and measured with a thermocouple contacting the outer surface of the injector. Measurements showed that for a reactor wall

temperature of 233 K, a constant temperature of 298 K could be maintained inside the injector. Under these conditions the temperature of the outer surface of the injector vacuum jacket was 280 K. As discussed below, we found that heating the injector was very important in minimizing complications associated with the production of BrO and HO₂ at low temperatures.

Mass spectrometric detection of reactants and products was carried out by continuous sampling at the downstream end of the flow tube through a three-stage differentially-pumped beam inlet system. The mass spectrometer (Extrel Model C50) consisted of an electron-impact ionizer, a quadrupole mass filter, and a channeltron detector. Beam modulation was accomplished with a 2001 Hz tuning fork type chopper placed inside the second stage of the mass spectrometer. Ion signals from the channeltron were sent to a lock-in amplifier that was referenced to the chopper frequency. The amplified analog signals were digitized (Analog Devices RTI/8 15) and recorded by a microcomputer.

Radical Production

In order to minimize systematic errors caused by unknown secondary reactions in the radical sources, the main flow tube and the reactor walls, we used several different reactions to produce BrO and HO₂ and the kinetic runs were carried out with both BrO and HO₂ as the excess reagent. The radical source conditions are summarized in Table 1 and described in detail below.

Two methods were used to produce BrO: (a) reaction of Br₂ with atomic oxygen generated by microwave discharge of O₂/He,



$$k_5(298 \text{ K}) = 1.4 \times 10^{-11} \text{ cm}^3 \text{ molecule}^{-1} \text{ s}^{-1} \quad (4)$$

and (b) reaction of ozone with bromine atoms generated in a microwave discharge of Br₂/He,



$$k_1 (298 \text{ K}) = 1.2 \times 10^{-12} \text{ cm}^3 \text{ molecule}^{-1} \text{ s}^{-1} (4)$$

For either of these source reactions, BrO radicals undergo rapid self-reaction, producing Br with about 85/0 efficiency at room temperature:



$$k_6 (298 \text{ K}) = 2.1 \times 10^{-12} \text{ cm}^3 \text{ molecule}^{-1} \text{ s}^{-1} (4)$$

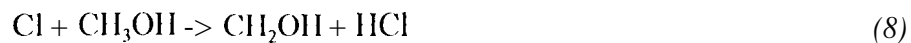
The highest concentrations of BrO were obtained using the Br+O₃ source in the presence of excess O₃. In this case, Br formed in reaction 6 was rapidly recycled back to BrO. For the Br+O₃ source, 4×10^{13} molecule cm⁻³ of Br₂ was flowed through a 1.27-cm-o.d. quartz discharge tube with 350 sccm helium carrier gas. After passing through the 30 cm-long central injector tube, $(1-10) \times 10^{14}$ molecule cm⁻³ of O₃ was introduced through the sidearm of the injector with 50 sccm of carrier helium gas, producing $(1-5) \times 10^{12}$ molecule cm⁻³ BrO radicals in the reactor. The O+Br₂ source was unable to produce BrO at these concentrations due to the lower microwave discharge efficiency of oxygen and BrO recombination, but this source was satisfactory for use in experiments where HO₂ was the excess reagent.

For the generation of HO₂, two separate methods were used: (a) reaction of hydrogen peroxide with atomic fluorine generated from microwave discharge of F₂,



$$k_7 (298 \text{ K}) = 4.98 \times 10^{-11} \text{ cm}^3 \text{ molecule}^{-1} \text{ s}^{-1} (13)$$

and (b) reaction of atomic chlorine from microwave discharge of Cl₂ with methanol followed by further reaction with oxygen,



$$k_8 (298 \text{ K}) = 5.4 \times 10^{-11} \text{ cm}^3 \text{ molecule}^{-1} \text{ s}^{-1} \quad (4)$$



$$k_9 (298 \text{ K}) = 9.1 \times 10^{-12} \text{ cm}^3 \text{ molecule}^{-1} \text{ s}^{-1} \quad (4)$$

As in our previous studies of HO₂ kinetics using this apparatus¹⁴, we found that method (a) was suitable for producing large concentrations of HO₂ at room temperature. Using the same sidearm arrangement as used for Br + O₃ with the quartz discharge tube replaced by an alumina tube, a small flow (5-20 seem) from a premixed So/O F₂/He cylinder was mixed with a larger (400 seem) helium flow which passed through the discharge. Dissociation of F₂ was typically greater than 90%. 11202 was added through the sidearm of the movable injector with 650 seem of carrier helium gas bubbling through the 90% 11202 solution. The reaction of F with H₂O₂ was completed within 1 ms and the initial F atom concentration, and thus the HO₂ concentration, was adjusted by varying the F₂ flow. About 10¹⁴ molecule cm⁻³ of H₂O₂ was brought into the injector, and the production of HO₂ in the reactor was initially in the range (1-8) x 10¹² molecule cm⁻³. This method was restricted to temperatures above 253 K due to condensation of H₂O₂ and H₂O on the flow tube walls which resulted in very high wall loss rates for HO₂.

Using method (b), chlorine atoms were formed by discharging a flow of 5-10 seem of 1% Cl₂ in helium to which was added an additional helium flow of 250-500 seem. Chlorine atoms reacted in the sidearm with CH₃OH obtained from a 5-10 sccm helium flow through a methanol saturator held at a pressure of 400 Torr and a temperature of 25 C. An oxygen flow of 20-40 seem was added along with the methanol. Using this method the highest HO₂ concentration that could be produced was ~1.5 x 10¹² molecule cm⁻³. The major difficulty with this method was that flowing a large quantity of methanol into the reactor created a large m/e = 33 background signal

which interfered with the HO₂ radical detection. This interference decreased substantially with decreasing methanol concentration. Thus for kinetics studies of reaction 3 with BrO in excess, method (b) was used to produce HO₂ as the minor reagent.

Both BrO and HO₂ radicals were detected using electron impact ionization mass spectroscopy at the parent peaks, m/e = 95 (BrO⁺) and m/e = 33 (HO₂⁺). When H₂O₂ was used as the HO₂ precursor, there was an m/e = 33 contribution arising from the fragmentation of H₂O₂ and from the wing of the much larger m/e 34 peak. This interference was minimized by optimizing the quadrupole resolution and the ionizer electron energy. Table 2 shows the m/e = 33 signal intensity as function of electron energy for the F⁺ + H₂O₂ system. It can be seen that the ratio of HO₂ signal to background m/e = 33 contribution was maximized at an electron energy of 19 eV, which was subsequently used in all kinetics studies.

Absolute concentrations of both BrO and HO₂ were calibrated by chemical conversion to NO₂ with excess NO, i.e.



This was accomplished by introducing the BrO or HO₂ radicals from the movable injector and NO from the sidearm of the reactor, with the injector placed in a downstream position such that the reaction time between NO and the calibrated radical was ≤ 3 ms. The concentration of added NO was in the range $(1-5) \times 10^{14}$ molecule cm⁻³. The conversion factors were determined from the ratio of the change in NO₂ ion signal at m/e 46, S₄₆, to the change in the radical signal, S₉₅ or S₃₃. ($\Delta S_{46}/\Delta S_{95} = 0.40 \pm 0.08$ and $\Delta S_{46}/\Delta S_{33} = 1.8 \pm 0.4$). The radical calibrations were then

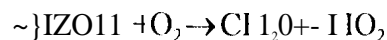
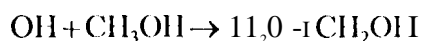
obtained from absolute calibrations of the mass spectrometer at m/e 46 using known concentrations of NO₂.

Special care was taken for the HO₂ calibration since HO₂ could be regenerated by the reactions,



$$k_{11} (298 \text{ K}) = 1.7 \times 10^{-12} \text{ cm}^3 \text{ molecule}^{-1} \text{ s}^{-1} (4)$$

or



One way to prevent this HO₂ regeneration in the titration was adding a large excess (~10¹⁵ molecule cm⁻³) of C₂F₃Cl which reacts rapidly with OH to form a stable adduct^{15,16}. However, it was found that this concentration of C₂F₃Cl reduced the responsivity of the mass spectrometer by ~6% due to a reduction in the efficiency of the ionizer. An alternative OH scavenger which had a negligible effect on the mass spectrometer was molecular bromine, Br₂. The reaction of Br₂ with OH is very fast,



$$k_{12} (298 \text{ K}) = 4.2 \times 10^{-11} \text{ cm}^3 \text{ molecule}^{-1} \text{ s}^{-1} (4)$$

thus when 5 × 10¹³ molecule cm⁻³ of Br₂ was introduced into the reactor, the OH radical was scavenged in less than 0.5 ms. The product of the OH + Br₂ reaction, HOBr, had no effect on the calibration. The detection limits for the radicals were 2 × 10⁹ molecule cm⁻³ for BrO and 8 × 10⁹ molecule cm⁻³ for HO₂ (S/N = 2 for a 10 s integration time.)

First-order wall loss coefficients were measured for both HO₂ and BrO and found to be less than 5 s⁻¹ at low radical concentrations (<5 × 10¹¹ molecule cm⁻³). For the runs with excess HO₂, the effective wall loss increased at the highest HO₂ concentrations, presumably due to the HO₂ self-reaction. As a first order approximation, the HO₂ concentration for the kinetic run was derived by averaging the concentrations at the upstream and downstream ends of the reaction zone. Simulations showed that the error arising from this approximation was ≤5%. In the case of excess BrO, the same procedure was employed although the wall loss was always less than 4 s⁻¹.

The gases used in this work had the following stated purities: He, 99.999%; NO, 99%; NO₂, 99.5% and Cl₂, (10% in He). F₂ (5% in He) and O₂ (99.999%). Br₂ (99.8%) was obtained and purified by vacuum distillation at 195 K. HO₂ was obtained commercially at a concentration of 70 wt % and purified to ≥ 94 wt % prior to use by vacuum distillation at room temperature. Ozone was produced by passing O₂ through an ozonizer and storing the product on silica gel at 195 K. During the experiments, O₃ was maintained at 195 K and evaporated into the reactor with a known flow of He. In order to avoid the potential explosion hazard associated with the condensation of ozone in the liquid nitrogen trap of the mechanical pump, efforts were made to decompose the ozone downstream of the flow tube. This was accomplished efficiently by heating the effluent from the flow tube to approximately 300 C in a 50-cm-long quartz tube containing copper scouring pads.

Results

Measurements of k_3 were carried out by monitoring the decay of either BrO or HO₂ as a function of reaction time. Bimolecular rate constants were obtained using the well-known steady state flow tube method,¹² in which the first-order decay rate constant, k'_3 , was determined from the slope of a plot of the logarithm of either BrO or HO₂ signal vs. reaction time. In all experiments the minor reactant was introduced into the flow tube through a fixed sidearm and the excess reagent was added through the sliding injector. In experiments in which HO₂ was the minor species, the signal was corrected by subtracting the m/e = 33 signal contribution from the HO₂ precursors as discussed above. In these experiments, the H₂O₂ concentration did not change appreciably with injector position as determined from measurements of the m/e 34 peak. The observed decays were then corrected for axial diffusion and for loss of BrO or HO₂ on the injector according to eq (1),]²

$$k'_{3,corr} = k'_3 \left(1 + \frac{k_p D}{v^2} \right) + k_p \quad (1)$$

where D is the diffusion coefficient, v is the mean bulk flow velocity, and k_p is the first order loss of BrO or HO₂ on the outside surface of the sliding injector (injector loss), Diffusion coefficient estimates were based on the data of Marrero and Mason.¹⁷ The estimated D values for BrO varied from 0.43 atm cm² s⁻¹ at 233 K to 0.84 atm cm² s⁻¹ at 348 K and for HO₂ varied from 0.49 to 0.97 atm cm² s⁻¹ over the same temperature range. The corrections for axial diffusion were always less than 10%.

Kinetics of BrO and HO₂ decay at 298 K. A typical BrO decay as function of the injector position at 298 K is shown in Figure 2. The BrO decay appeared to be linear within the time domain studied, and the BrO was completely titrated to our detection limit at high HO₂ concentrations ([HO₂] ≥ 5 × 10¹² molecule cm⁻³). With initial BrO concentrations of (2-5) × 10¹¹

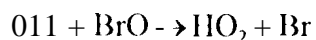
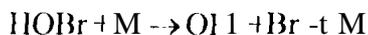
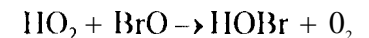
molecule cm^{-3} and HO_2 concentrations of $(1-8) \times 10^{12}$ molecule cm^{-3} , the dependence of k'_3 on $[\text{HO}_2]$ is shown in Figure 3. k'_3 varied from 20 to 160 s^{-1} in the HO_2 concentration range of interest. Figure 3 also shows the results of measurements of k'_3 taken over a range of flow velocities and total pressures to check for the presence of systematic errors such as bimolecular wall reactions. For flow velocities of 750-1800 cm s^{-1} and total reactor pressures of 1-3 Torr the first-order decay of BrO due to reaction with HO_2 was independent of these parameters. From the slope of linear least squares fit through all the data at 298 K, k_3 was determined to be $(1.73 \pm 0.61) \times 10^{-11}$ $\text{cm}^3 \text{ molecule}^{-1} \text{ s}^{-1}$, where (and hereafter) the quoted uncertainty is at the 95% confidence level and includes both random and systematic errors.

The behavior of HO_2 in the presence of excess BrO was also investigated. Figure 4 shows a typical HO_2 decay as function of injector position over the BrO concentration range $(1.3-4.5) \times 10^{12}$ molecule cm^{-3} at 298 K. Twenty four runs were performed at 298 K and the bimolecular rate coefficient for reaction 3 in excess BrO was derived as $(2.05 \pm 0.64) \times 10^{-11}$ $\text{cm}^3 \text{ molecule}^{-1} \text{ s}^{-1}$ from a linear least-squares fit to the data in Figure 5.

Temperature dependence of the rate coefficient for reaction 3. Rate constants for reaction 3 were measured over the temperature range 233-348 K using both excess BrO and excess HO_2 with the source reactions and inlet conditions shown in Table 1. Both secondary reactions and wall reactions limited the temperature range of the study. These complications will be discussed in detail below.

At temperatures between 298 K and 348 K, both the BrO (excess reagent, $\text{Br} + \text{O}_3$ source) and HO_2 (minor reagent, $\text{Cl} + \text{Cl}_2$ source) ion signals were well-behaved with no significant complications. Above 348 K, there was significant regeneration of HO_2 as indicated by the $m/e =$

33 ion signal reaching a steady-state at long reaction times ($t > 65$ ms). A possible explanation for this behavior is secondary production of HO_2 arising initiated by the thermal decomposition of HOBr :



This effect limited to 348 K the maximum temperature for which reliable kinetics results could be obtained.

At temperatures below 298 K, a number of processes interfered with the production of both BrO and HO_2 . For HO_2 produced using the $\text{F} + \text{H}_2\text{O}_2$ source, the maximum concentration that could be achieved decreased significantly below about 270 K. The dependence of the observed $m/e = 33$ signal on temperature is shown in Figure 6. For these experiments, HO_2 was produced in an unheated injector and the temperature was measured in the flow tube jacket which was not in thermal equilibrium with the injector due to the time lag in cooling and heating. The observed signal decrease in the cooling cycle and increase in the heating cycle are attributed to adsorption and desorption of H_2O and HO_2 on the flow tube and injector walls. The decrease in the HO_2 concentration is due to both an increase in the HO_2 wall loss rate on the coated surfaces and the removal of H_2O_2 from the gas phase. The use of the heated injector eliminated these problems in the injector itself, but deposition of H_2O and HO_2 on the flow tube walls remained a problem at temperatures below 253 K. As in the experiments of Larichev et al., we observed that the $\text{Cl} + \text{CH}_3\text{OH} \rightarrow \text{H}_2\text{O} + \text{O}_2$ source efficiency decreased rapidly at temperatures below about 250 K in the unheated injector. Larichev et al. dealt with this problem by moving their HO_2 source reactor to a sidearm in the uncooled region of the flow tube, but since HO_2 was the excess reagent in

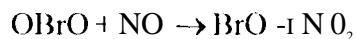
their experiments, this introduced the first-order BrO wall loss into their observed decay rates. In our experiments at low temperatures, 1102 was the minor reagent and the Cl+CH₃OH+O₂ source could be used in the sidearm at room temperature without requiring a separate measurement of the wall loss.

The temperature dependence of the BrO⁺ ion signal using the O + Br₂ source in the sidearm is shown in Figure 7. As in the case of 1102, the BrO concentration in the flow tube displays a hysteresis in the cooling/warming cycle indicating the presence of complex wall reactions. Observation of the flow tube surface at low temperature revealed a solid layer on the injector surface with a white-yellow color. This layer was observed using both the O + Br₂ and Br + O₂ sources. We further studied this solid layer using the heated injector. This was carried out by cooling the injector for one hour with the BrO source on, then switching off the source and warming the injector while scanning the mass spectrometer for desorption products. Three major species were simultaneously detected at m/e = 95/97 (BrO⁺), m/e = 111/113 (OBrO⁺ or BrOO⁺), and m/e = 174 (Br₂O⁺), which peaked at injector temperatures of -260 K, 270 K, and 280 K, respectively. Parent mass peaks corresponding to other higher oxides such as Br₂O₂, Br₂O₄ or Br₂O₇ could not be detected but if these species were formed, they would likely have fragmented and contributed to the daughter fragments indicated above.

Higher bromine oxides have been observed several times previously in discharge-flow/mass spectroscopy studies of oxygen-bromine systems^{8,18}. The detailed formation mechanisms are not known but wall reactions play a key role in the formation and interconversion of the bromine oxides, and the primary products may be both OBrO and Br₂O¹⁹. The surface reactions appear to require the presence of O(³P) and/or metastable oxygen

$O_2(^1\Delta, ^1\Sigma)$ from the microwave discharge. In order to characterize the products of the wall reactions occurring in the flow reactor, separate experiments were carried out using similar discharge-flow systems coupled to UV-visible and submillimeter absorption spectrometers²⁰. In both systems, the product of an O_2 discharge reacted with a flow of Br_2 at low temperature (-20 °C) to form the same yellow-white solid observed in the DF/MS apparatus. The vapor from the solid was recorded by the spectrometers after the deposition of the solid was discontinued. In the UV/visible apparatus, an intense progression of vibrational bands was observed in the 380-620 nm spectral region which was nearly identical to the spectrum observed by Rattigan et al. in the steady-state photolysis of Br_2-O_3 mixtures and assigned to $OBrO$ ²¹. In the submillimeter spectrometer, a large number of rotational lines were observed²². Analysis of the spectra identified the source of the lines as isotopomers of both $OBrO$ and Br_2O .

Adding NO to the desorbing species resulted in the formation of NO , most likely from the $NO + OBrO$ reaction:



Under conditions where the bromine oxides were formed (low temperature, $O + Br_2$ source, unheated injector) this reaction interfered with the mass spectrometric calibration of BrO .

When the resistively heated injector was used, most of the problems associated with the low-temperature production of BrO and HO_2 were eliminated, and this system was used for all of the low temperature studies. The wall loss of radicals at low temperatures was examined with the heated injector. The first-order BrO wall loss was negligible down to 210 K but the HO_2 wall loss increased significantly with decreasing temperature. As shown in Figure 8, the HO_2 wall loss was $\sim 7 s^{-1}$ at 298 K, increasing to $64 s^{-1}$ at 213 K. The large wall loss rate of HO_2 at low

temperature restricted the range of reliable kinetics measurement for reaction 3 to 233 K and above.

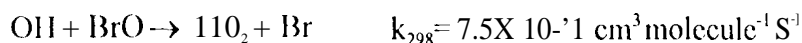
Kinetics data were obtained over the temperature ranges 233-348 K with BrO in excess and 253-298 K with HO₂ in excess. The rate constant data are summarized in Table 3 and an Arrhenius plot is shown in Figure 9. From these data it is apparent that the rate coefficient has a negative temperature dependence. For the three temperatures at which both excess BrO and excess HO₂ data are available, the rate constants using excess BrO are systematically 20-25% larger, but the data overlap within the $\pm 2\sigma$ error limits. Although the data show a small non-linear Arrhenius temperature dependence, the curvature lies well within the uncertainty of the measurements. A linear least-squares fit gives the following Arrhenius expression:

$$k_3 = (3.13 \pm 0.33) \times 10^{-2} \exp(536 \pm 206/T).$$

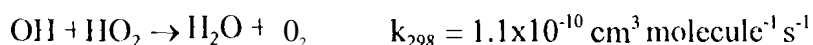
The reaction products for BrO + HO₂ were briefly studied with HO₂ in excess. HOBr was found to be the predominant reaction product based on approximate absolute mass spectrometric calibrations of HOBr. Small 11Br mass peaks were also detected at 298 K, but it was not possible to ascribe them to the 11Br formation channel of reaction 3 since other processes such as Br + HO₂ and Br + H₂O₂ and wall reactions could also contribute to 11Br formation..

Discussion

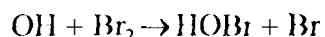
Effects of Secondary Reactions. The agreement (within 20%) between rate coefficients obtained under excess HO₂ and excess BrO conditions shows that, in general, there are no significant complications from secondary reactions. There are a few processes that need to be considered explicitly, however. The reaction



has been studied recently by Bogan et al.²³ and found to be significantly faster than previously estimated. In the kinetic runs which used excess HO₂, simulations show that an OH impurity equal to about 0.2 [HO₂], could effectively double the observed first-order disappearance rate of BrO under conditions where there are no other removal paths for OH. In our system, OH is formed in the HO₂ source as a result of the reaction of fluorine atoms with water vapor which is present as an unavoidable impurity in H₂O₂. conditions in the source are adjusted in the H₂O₂ source to allow the fast reaction

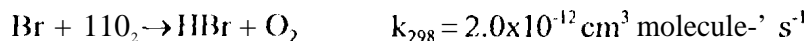


to scavenge most of the OH on the time scale of the source chemistry. The HO₂ source should therefore be a negligible source of OH (less than 1 × 10¹⁰ cm³ molecule⁻¹ s⁻¹ in the flow tube). In addition, Br₂ is present at concentration around 10¹³ molecule cm⁻³ from the BrO source. This concentration of Br₂ is sufficient to scavenge OH rapidly from the reaction



as discussed above. The absence of significant impurity concentrations of OH from the HO₂ source was verified in separate experiments which set a conservative upper limit of 10¹⁰ molecule cm⁻³ for HOBr when the HO₂ source was on and the BrO discharge was off.

The reaction



is a potential secondary removal pathway for HO₂ in the excess BrO experiments because the BrO + BrO reaction is a source of Br in the flow tube. Simulations show that most of the Br

reacts with O_3 , which regenerates BrO and suppresses the concentration of Br to the point where removal of HO_2 by Br can be neglected.

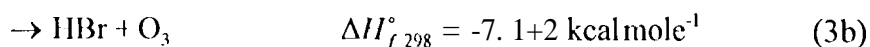
Comparison of Results with Previous Studies: The results of previous kinetics studies of the $HO_2 + BrO$ reaction are summarized in Table 4 and in Figure 9. The measured values of k_{298} fall into three groups: the early measurement of Cox and Sheppard at $5 \times 10^{-12} \text{ cm}^3 \text{ molecule}^{-1} \text{ s}^{-1}$, the considerably higher values around 3.3×10^{-11} from Poulet et al., Larichev et al. and Bridier et al., and the intermediate values in the range $(1.4-2.0) \times 10^{-11} \text{ cm}^3 \text{ molecule}^{-1} \text{ s}^{-1}$ from Elrod et al. and this work. The significant difference between the results from this work and the two studies of the Orleans group is puzzling because both groups used discharge-flow/mass spectroscopy systems at low pressure with similar radical sources. There are, however, some differences in methodology which may account for the disagreement. Both studies used the $Cl + CH_3OH$ reaction to produce HO_2 . This source is strongly affected by wall reactions below about 250K as observed in both studies. Larichev et al. dealt with this problem by producing HO_2 in a sidearm at room temperature in the flow tube. This approach eliminates problems associated with the reduced efficiency of the source at low temperature, but since the excess reagent (HO_2) is not injected from the moveable inlet, the first-order wall loss of HO_2 contributes to the measured first-order rate constant. Complications associated with the $Cl + Cl_2O$ source at low temperatures were circumvented in the present study by always keeping the sliding injector source at room temperature using the integral heating coil. This approach maintains the advantage of introducing the excess reagent through the sliding injector.

The values of k_{298} obtained in the three temperature dependence studies range over a factor of about 2.4 but the measured values of E/R are remarkably similar as seen in Table 4. All three studies report a moderately negative temperature dependence with the values ranging from

-520 to -580 K⁻¹. In the study of Larichev et al., the measurement of k_3 at 233 K was not considered in the determination of E/R because it fell considerably off the Arrhenius line described by their 243-344 K data. In the present work the Arrhenius plot was linear over the 233-348 K temperature range, and in the study of Elrod et al. the plot was linear over the range 210-298 K.

Reaction Mechanism: The mechanism for the formation of IOX from HO₂ + XO, where X=Cl or Br, has not been established with certainty but *ab initio* calculations are available which provide estimates of the stabilities of the possible reaction intermediates. In the system involving Cl, Francisco and Sander calculated enthalpies of formation for several ICLO₃ isomers using both isodesmic reactions at the Q-ISIS(1')16-311 G(2df,2p) level and G1/G2 theory²⁴. Values of $\Delta H_{f,0}^\circ$ (in kcal mole⁻¹) were determined to be HOClO₂ (4.2), HOOOCl (9.1), HOOCIO (25) and ICLO₃ (46.1). For IOOCIO and HOOOCl these results are significantly different from the values obtained from the bond additivity calculations of Stimpfle et al.²⁵. The most stable isomer, HOClO₂ is unlikely to form from HO₂ + ClO because of the extensive rearrangement required. The next most stable intermediate, HOOOCl, is the likely intermediate in the reaction pathway leading to HCl through formation of a five-membered transition state followed by HCl elimination, however, the small branching ratio measured for this pathway implies the existence of a significant exit channel barrier²⁶⁻²⁸. The likely intermediate in the formation of HOCl is HOOCIO as suggested by Stimpfle et al.²⁵ because the observed negative temperature dependence is more consistent with a mechanism involving a strongly bound intermediate (IOOCIO) than the weakly bound intermediate involved in hydrogen abstraction (ClOHOO).

The thermochemistry of the $\text{BrO} + \text{HO}_2$ system is qualitatively similar to its chlorine counterpart. The $\text{BrO} + \text{HO}_2$ reaction has several exothermic reaction pathways:



where $\text{HO}_2 \cdot \text{BrO}$ denotes a collisionally stabilized adduct. Several previous studies including the present work found that reaction 3a was an important, if not the predominant, reaction channel but were not able to establish that the branching ratio for reaction 3a was unity.^{8,10} On the other hand, there is positive evidence that the branching ratio for reaction 3b is quite small. Larichev et al. were unable to detect O_3 in their study of reaction 3 and set an upper limit of 0.015 for $\frac{k_{3b}}{k_3}$ over the temperature range 233-298 K. Mellouki et al. inferred an upper limit of 1×10^{-4} for $\frac{k_{3b}}{k_3}$ at 300 K based on studies of the reverse reaction,



using laser magnetic resonance detection of HO_2 .²⁹ There have been no indications from any previous study that reaction 3 results in the formation of a stable adduct as indicated in reaction 3c. *Ab initio* calculations by Guha and Francisco³⁰ at the 1131.YP/6-311++G(3df,3pd) level show that the enthalpies of formation of HBrO_3 isomers increase in the order HOBrO_2 : HOOOBr : $\text{HO}^{\circ}\text{BrO}$: HBrOOO . This is the same ordering as the analogous system involving chlorine. While absolute energies for HBrO_3 isomers are not yet available, it is clear from the observed negative temperature dependence of the HOBr channel that potential energy surfaces are qualitatively similar to the chlorine system. The 298 K rate constants for the $\text{HO}_2 +$

XO reactions increase significantly as X is substituted in the order Cl:Br:I. *Began et al.* have attributed this to the increasing tendency of the larger XO species to access the available triplet surfaces through spin-orbit coupling 23. Other factors that may contribute to the observed rate constant enhancement are stronger long-range interactions between HO₂ and XO, and progressive loosening of the HOOXO transition state.

Atmospheric Implications:

The combined results of this study and the work of *Elrod et al.* strengthen the case for a smaller rate coefficient for reaction 3 than the value that appears in the 1994 NASA Data Evaluation. This will have the effect of slightly lowering the overall catalytic destruction rate of ozone by bromine, and consequently the ozone depletion potential of CH₃Br. The reduction in k_3 will have the effect of repartitioning bromine from HOBr into BrO, which will increase the rate of the BrO + ClO cycle, partially offsetting the effect on the HO₂ + BrO cycle.

Summary

We have studied the kinetics of the reaction of BrO with HO₂ over the temperature range 233-348 K using the technique of discharge flow/mass spectrometry. Variations in experimental conditions such as flow velocity, reactor total pressure, and the excess reactant (HO₂ or M-O) had no effect on the measured rate coefficients within the 2 σ error limits. At 298 K, the rate coefficient was determined to be $(1.73 \pm 0.61) \times 10^{-11} \text{ cm}^3 \text{ molecule}^{-1} \text{ s}^{-1}$ with HO₂ in excess and $(2.05 \pm 0.64) \times 10^{-11} \text{ cm}^3 \text{ molecule}^{-1} \text{ s}^{-1}$ with BrO in excess, respectively. The combined data from the excess BrO and excess HO₂ experiments were fit to an Arrhenius expression which gave $k_3 =$

$(3.13 \pm 0.33) \times 10^{12} \exp(536 \pm 206/T)$. These results obtained here, along with the measurements of Hirod et al. contrast with three recent studies giving 298 K rate constants that are about a factor of two larger. The reasons for the discrepancy are not well understood.

Acknowledgement

This research was performed by the Jet Propulsion Laboratory, California Institute of Technology, under contract with National Aeronautics and Space Administration. We are grateful to J. S. Francisco and S. Guha for providing details of their *ab initio* calculations on HBrO_3 , and to David Natzic and Juergen Linke for their expert technical assistance in this work.

References

- 1 WMO, 'Scientific Assessment of Ozone Depletion: 1994', National Aeronautics and
Space Administration, 1994.
- 2 S. C. Wofsy, M. B. McElroy, and Y. L. Yung, *Geophys. Res. Lett.*, 1975, **2**, 215.
- 3 Y. L. Yung, J. P. Pinto, R. 'I'. Watson, and S. I'. Sander, *J. Atmos. Sci.*, 1980, **37**, 339.
- 4 W. B. DeMore, D. M. Golden, R. F. Hampson, C. J. Howard, M. J. Kurylo, M. J. Molina,
A. R. Ravishankara, and S. P. Sander, in 'Chemical Kinetics and Photochemical Data for
Use in Stratospheric Modeling', Pasadena, CA, 1994.
- 5 R. Atkinson, D. L. Baulch, R. A. Cox, R. F. Hampson, J. A. Kerr, and J. Troe, *J. Phys.*
Chem. Ref. Data, 1992, **21**, 1125.
- 6 R. A. Cox and D. W. Sheppard, *J. Chem. Soc. Faraday Trans. 2*, 1982, **78**, 1383.
- 7 G. Poulet, M. Pirre, F. Maguin, R. Ramaroson, and G. Le Bras, *Geophys. Res. Lett.*,
1992, **19**, 2305.
- 8 M. Larichev, F. Maguin, G. Le Bras, and G. Poulet, *J. Phys. Chem.*, 1995, **99**, 15911.
- 9 I. Bridier, B. Veyret, and R. Lesclaux, *Chem. Phys. Lett.*, 1993, **201**, 563.
- 10 M. J. Elrod, R. F. Meads, J. B. Lipson, J. V. Secley, and M. J. Molina, *J. Phys. Chem.*,
1996, **100**, 5808.
- 11 G. W. Ray, L. F. Keyser, and R. T. Watson, *J. Phys. Chem.*, 1980, **84**, 1674.
- 12 R. R. Friedl and S. P. Sander, *J. Phys. Chem.*, 1989, **93**, 4756.
- 13 C.-D. Walther and I. G. Wagner, *Ber. Bunsenges. Phys. Chem.*, 1983, **87**, 403.
- 14 S. P. Sander, *J. Phys. Chem.*, 1984, **88**, 6018.
- 15 C. J. Howard, *J. Chem. Phys.*, 1976, **65**, 4771.
- 16 J. P. D. Abbatt and J. G. Anderson, *J. Phys. Chem.*, 1991, **95**, 2382.
- 17 T. R. Marrero and F. A. Mason, *J. Phys. Chem. Ref. Data*, 1972, **1**, 3.
- 18 N. I. Butkovskaya, I. I. Morozov, V. J. Talrose, and E. S. Vasiliev, *Chem. Phys.*, 1983,
79, 21.
- 19 O. V. Rattigan, R. A. Cox, and R. L. Jones, *J. Chem. Soc. Faraday Soc. Trans.*, 1995, **91**,
4189.
- 20 C. E. Miller, S. L. Nikolaisen, and S. I'. Sander, *manuscript in preparation*.
- 21 O. V. Rattigan, R. L. Jones, and R. A. Cox, *Chem. Phys. Lett.*, 1994, **230**, 121.

- 22 11. S. P. Mueller, C.F. Miller, and E. A. Cohen, *Angewandte Chemie*, 1996, **35**, 2005.
- 23 D. J. Bogan, R. P. Thorn, F. I. Nesbitt, and L. J. Stief, *J. Phys. Chem.*, 1996, 100, 14383.
- 24 J. S. Francisco and S. P. Sander, *J. Phys. Chem*, 1996, 100, 573.
- 25 R. Stimpfle, R. Perry, and C. J. Howard, *J. Chem. Phys.*, 1979, 71, 5183.
- 26 M. T. Lcu, *Geophys. Res. Lett.*, 1980, 7, 173.
- 27 P. J. Leck, J. E. Cook, and J. W. Birks, *J. Chem. Phys.*, 1980, 72, 2364.
- 28 M. Finkbeiner, J. N. Crowley, O. Ilorie, R. Muller, G. K. Moortgat, and P. J. Crutzen, *J. Phys. Chem.*, 1995, 99, 16264.
- 29 A. Mellouki, R. K. Talukdar, and C. J. Howard, *J. Geophys. Res.*, 1994, **99**, 22949.
- 30 S. Guha and J. S. Francisco, private communication.

Table 1. Summary of Radical Source Reactions and Reactor Conditions for the BrO+HO₂ Reaction.

Radical	Reagent Stoichiometry	Source Reaction(s)	Source Location	Flow Tube Temperature	Concentration (10 ¹² molecule cm ⁻³)
HO ₂	excess	F + H ₂ O ₂	injector	253-298	1-8
HO ₂	minor	Cl + CH ₃ OH	sidearm	233-348	0.1-1.5
BrO	excess	Br + O ₃	injector	233-348	1-5
BrO	minor	O + Br ₂	sidearm	253-298	0.1-0.5

Table 2. Signal (rev) at m/e = 33 as a Function of Ionizer Electron Energy for the F+H₂O₂ system.

Signal Source	Ionizer Electron Energy (ev)									
	25	24	23	22	21	20	19	18	17	
(a) Signal from F + H ₂ O ₂	643	510	473	365	300	220	155	85	35	
(b) Signal from H ₂ O ₂ alone	230	170	115	79	48	29	15	8.6	4.0	
$\frac{(a) - (b)}{(b)}$	1.8	2.0	3.1	3.6	5.3	6.6	9.3	8.9	7.8	

[†]Emission current was 1.0 ma.

Table 3. Summary of Experimental Conditions and Measured Rate Constants for the Reaction $\text{HO}_2 + \text{BrO} \rightarrow \text{Products}$.

Pressure (Torr)	Temperature (K)	$k_3 \times 10^{11}$ ($\text{cm}^3 \text{ molecule}^{-1} \text{ s}^{-1}$)	Excess Reagent
1	348	1.35 ± 0.44	BrO
1	323	1.76 ± 0.52	BrO
1	298	2.05 ± 0.64	BrO
1-3	298	1.73 ± 0.61	HO_2
1	273	2.62 ± 0.87	BrO
1	273	2.06 ± 0.62	HO_2
1	253	2.80 ± 1.11	BrO
1	253	2.32 ± 0.65	HO_2
1	233	3.06 ± 1.15	BrO

Table 4. Comparison of Rate Constant Measurements for the Reaction $\text{HO}_2 + \text{BrO} \rightarrow \text{Products}$

Reference	Technique	Pressure (Torr)	Temperature (K)	$k_3 \times 10^{11}$ ($\text{cm}^3 \text{ molecule}^{-1} \text{ s}^{-1}$)
Cox and Sheppard ⁶	MP/UV	760	303	$0.5^{+0.5}_{-0.3}$
Poulet et al. ⁷	DF/MS	1	298	3.3 ± 0.5
Bridier et al. ⁹	FP/UV	760	298	3.4 ± 1.0
Larichev et al. ⁸	DF/MS	1	233-344	$(0.48 \pm 0.03) \exp[(580 \pm 100)/T]$
Elrod et al. ¹⁰	DF/MS	100	210-298	$(0.25 \pm 0.08) \exp[(520 \pm 80)/T]$
This Work	DF/MS	1	233-348	$(0.31 \pm 0.03) \exp[(540 \pm 210)/T]$

Figure Captions:

Figure 1. Experimental apparatus arrangement for kinetics study of BrO + HO₂.

Figure 2. BrO decay in the presence of excess HO₂ at 298 K. HO₂ was produced using the F + I₂O₂ source. HO₂ concentrations are in units of 10¹² molecule cm⁻³.

Figure 3. First-order decay rate of BrO, k_3' , as a function of [HO₂] at 298 K. (○) P_{total} = 1 Torr and v = 750 cm s⁻¹, (◊) P_{total} = 1 Torr and v = 1600 cm s⁻¹, (△) P_{total} = 3 Torr and v = 1800 cm s⁻¹, (—) best fit.

Figure 4. HO₂ decay in the presence of excess BrO at 298 K. BrO was produced using the Br + O₃ source. BrO concentrations are in units of 10¹² molecule cm⁻³.

Figure 5. First-order decay rates, k_3' , of HO₂ as a function of [BrO] at 298 K (△), 253 K (○), and 348 K (◊).

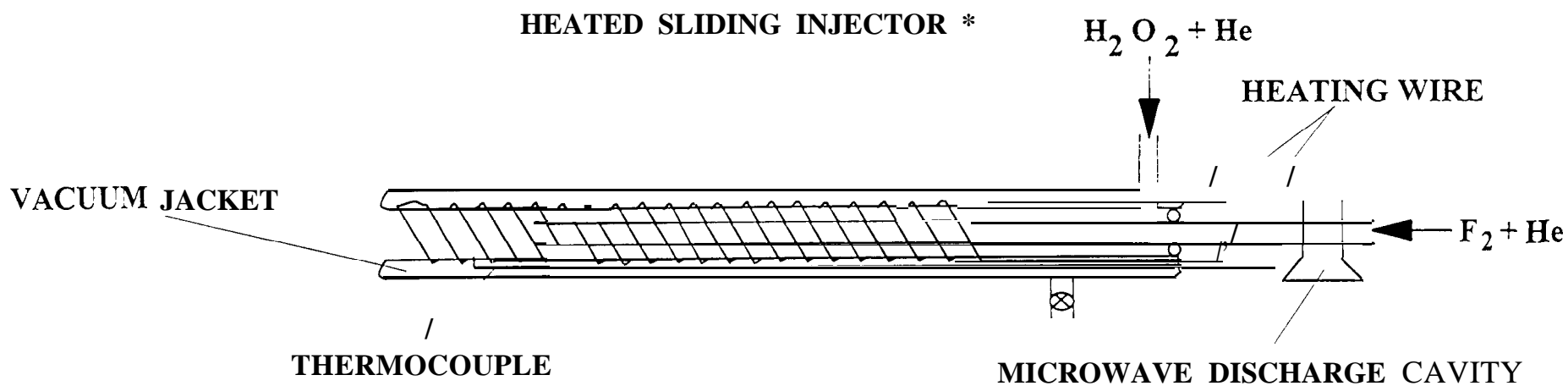
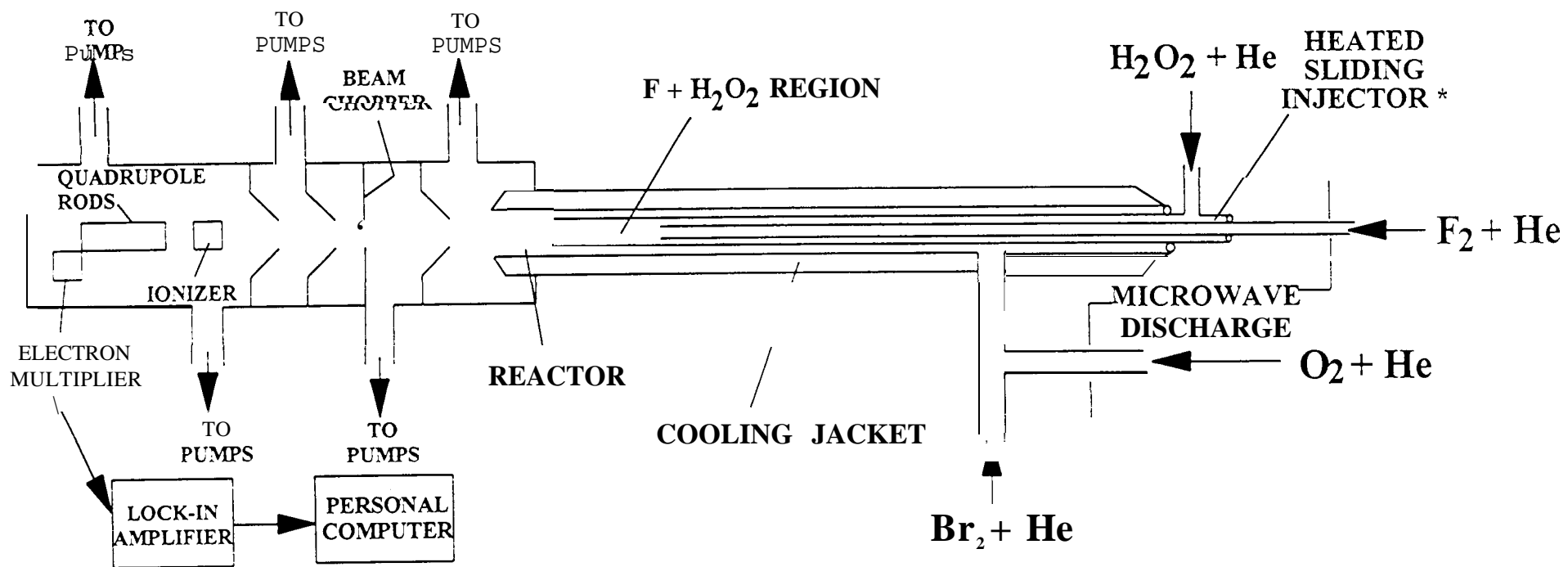
Figure 6. HO₂ signal intensity as a function of flow tube temperature using the F + I₂O₂ source, (○) cool-down, (◻) warm-up.

Figure 7. BrO signal intensity as a function of flow tube temperature using the O + Br₂ source, (○) cool-down, (◻) warm up.

Figure 8. Effective wall loss rate constant for HO₂ as a function of reactor temperature (○) 298 K, (◻) 273 K, (△) 253 K, (▽) 233 K, (◊) 213 K.

Figure 9. Temperature dependence of the rate constant for the BrO + HO₂ reaction: (○) this work, excess HO₂; (◻) this work, excess BrO; (●) Poulet *et al.* 7; (▽) Larichev *et al.* 8; (◊) Bridier *et al.* 9; (◻) Elrod *et al.* 10; (—) best fit to data from this work.

EXPERIMENTAL APPARATUS FOR KINETICS STUDY OF $\text{BrO} + \text{HO}_2$



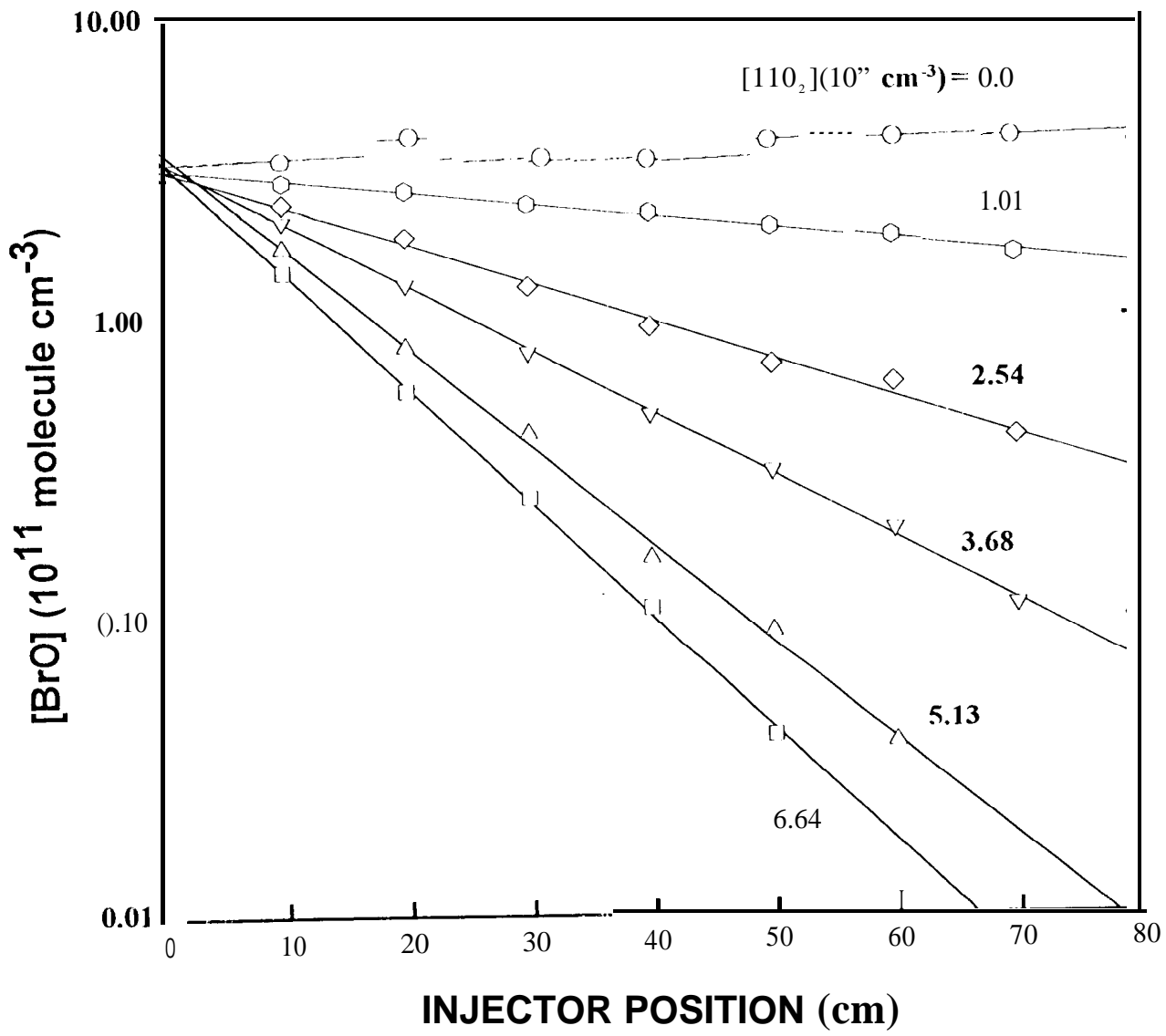
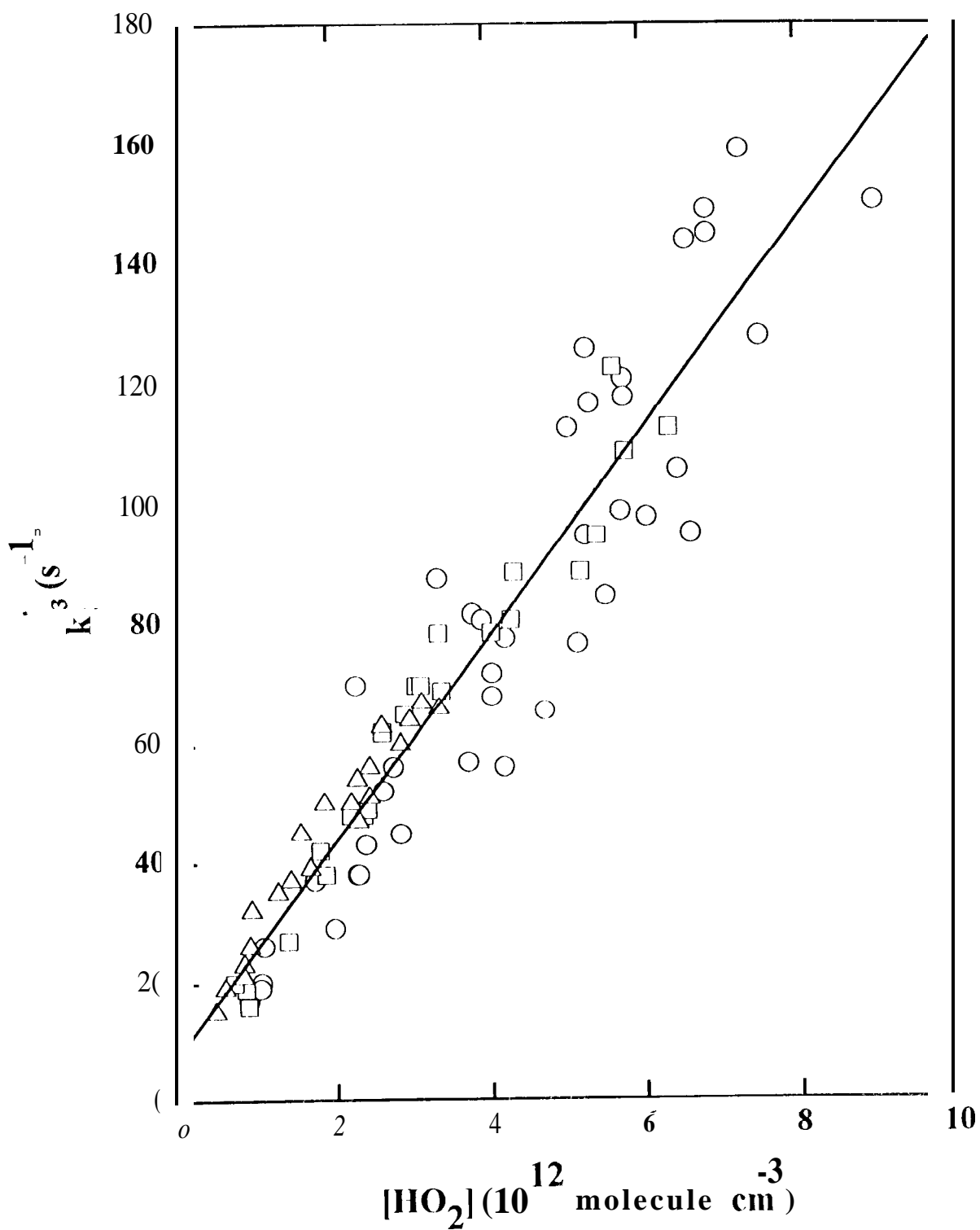


Figure 2



6 - 100

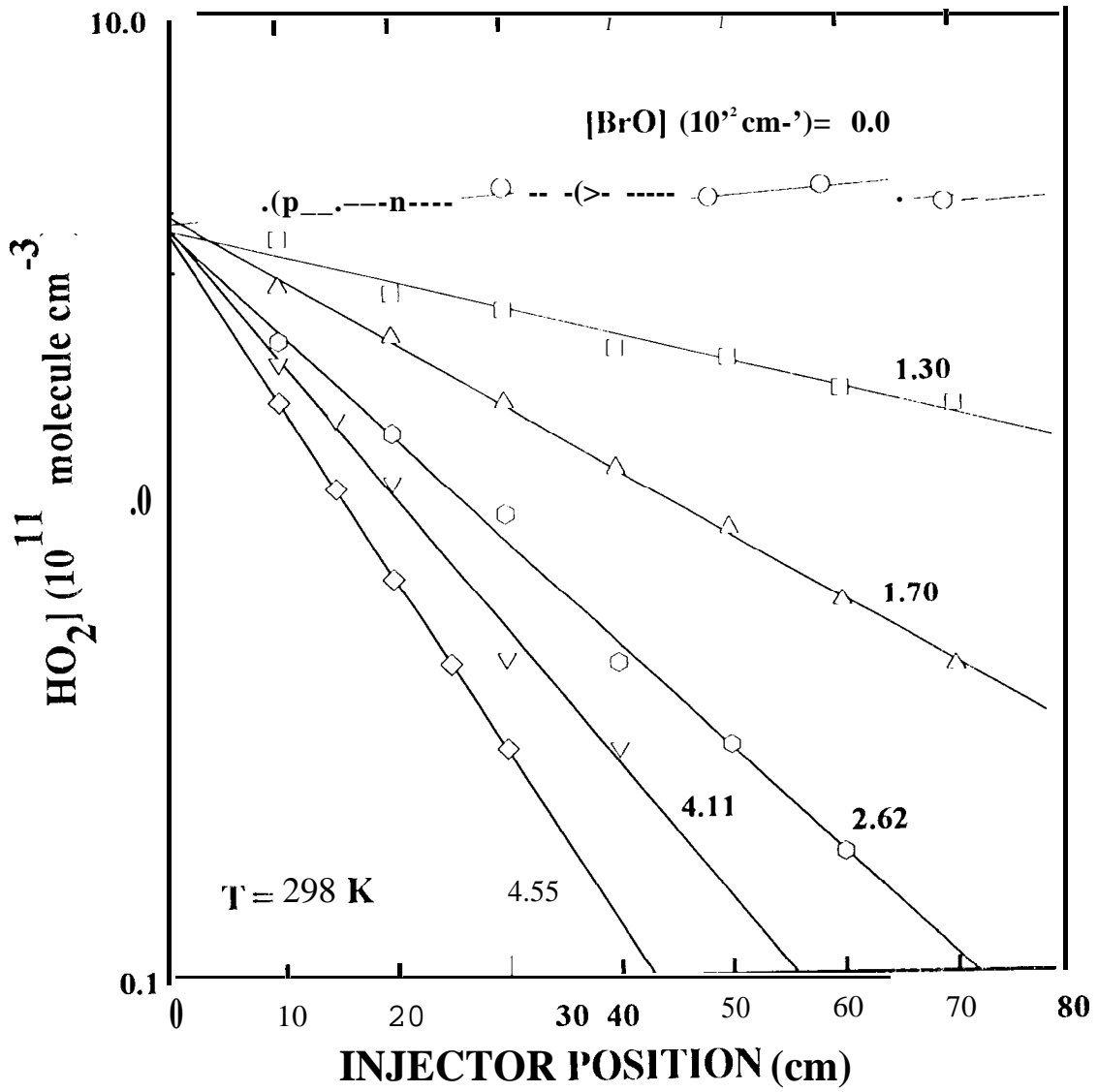
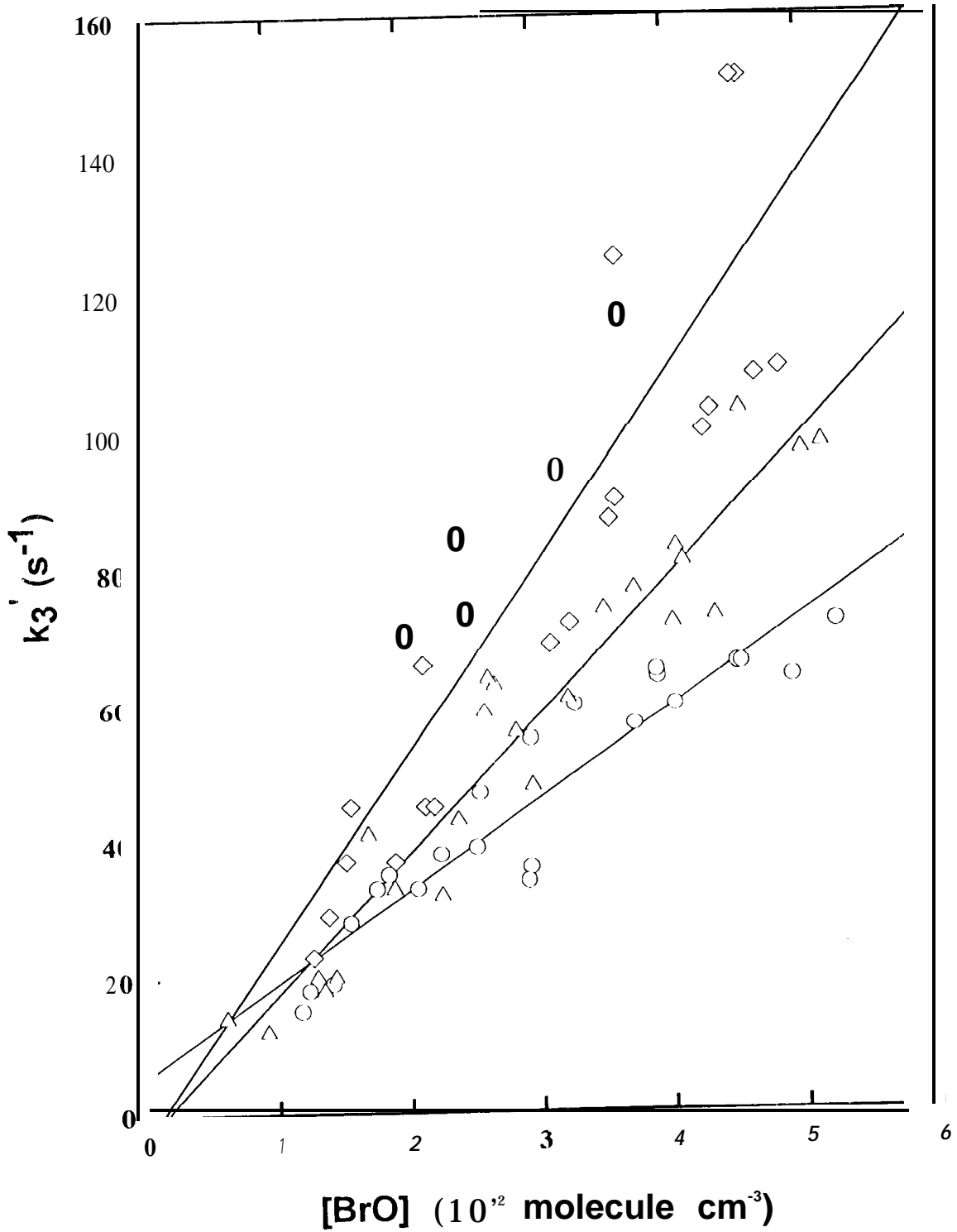


Figure 4



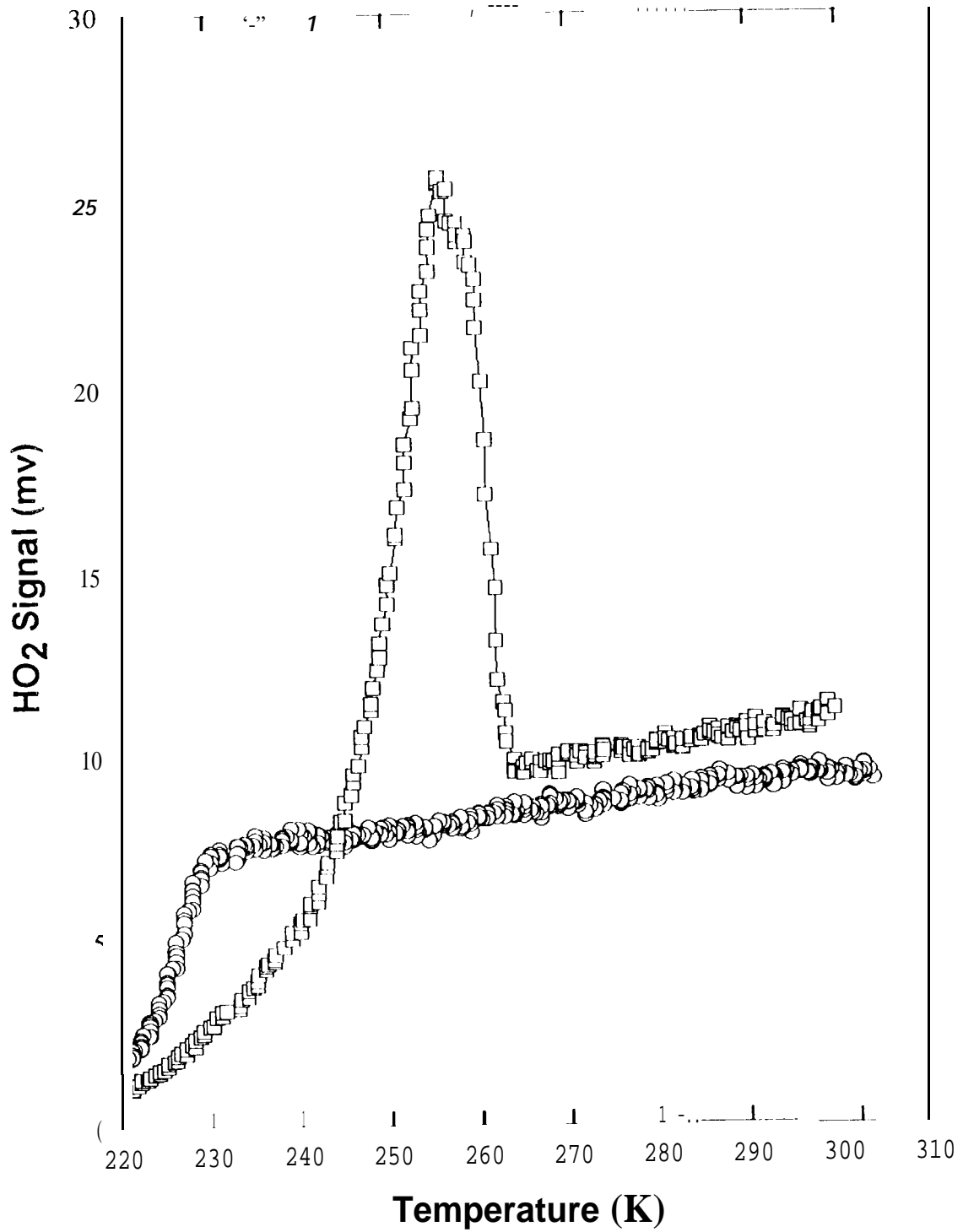


Figure 6

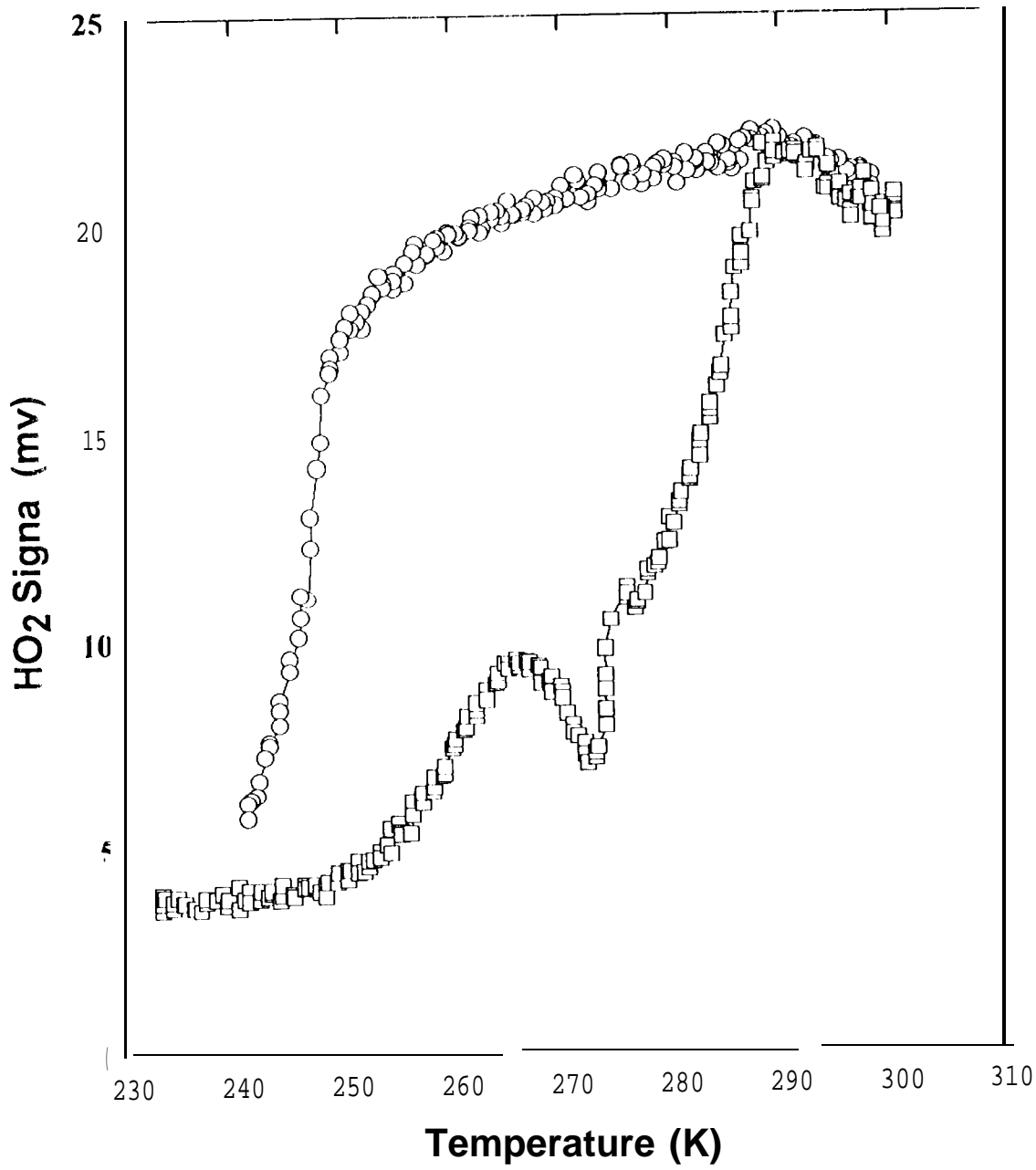


Figure 1

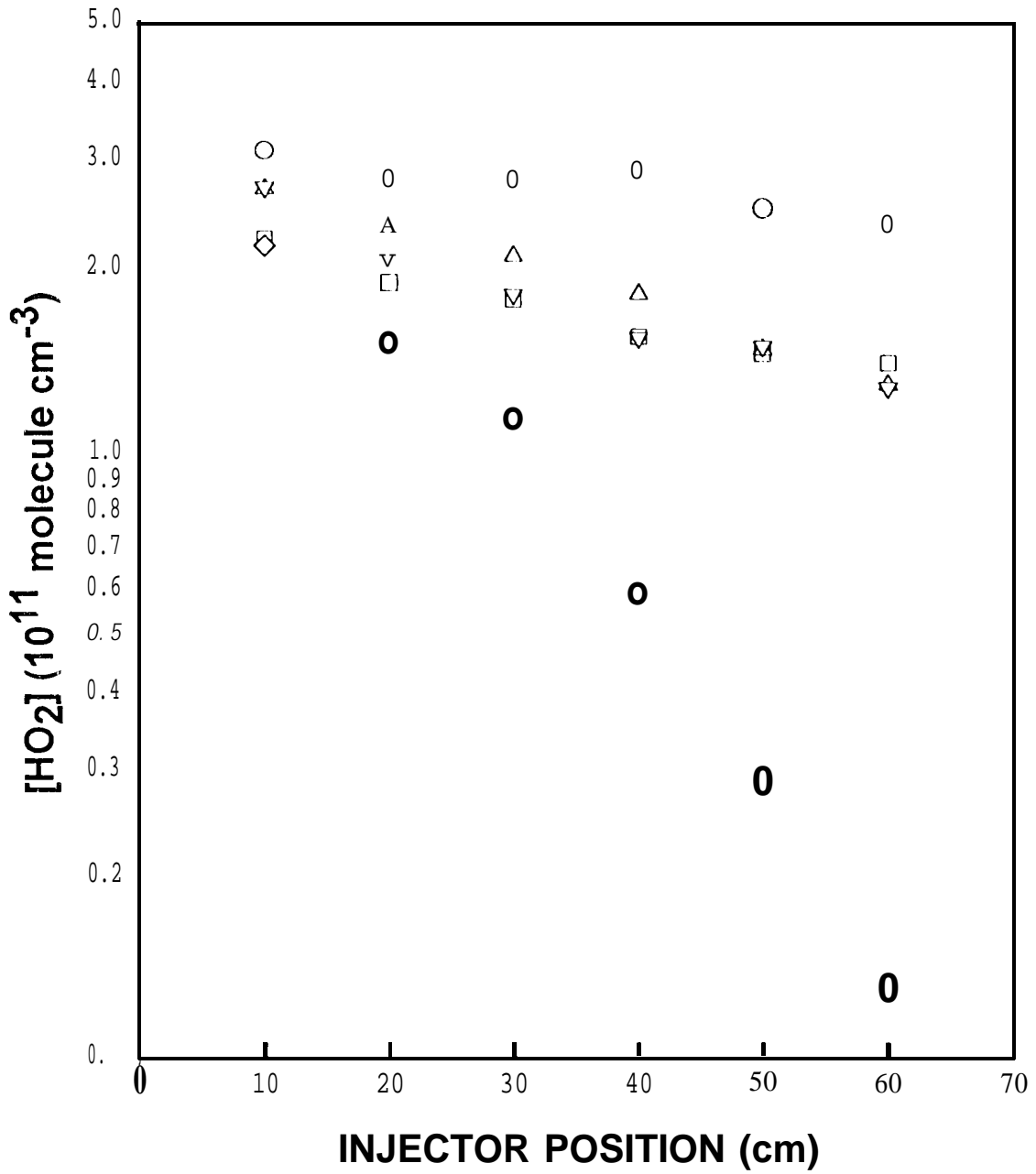


Figure 8

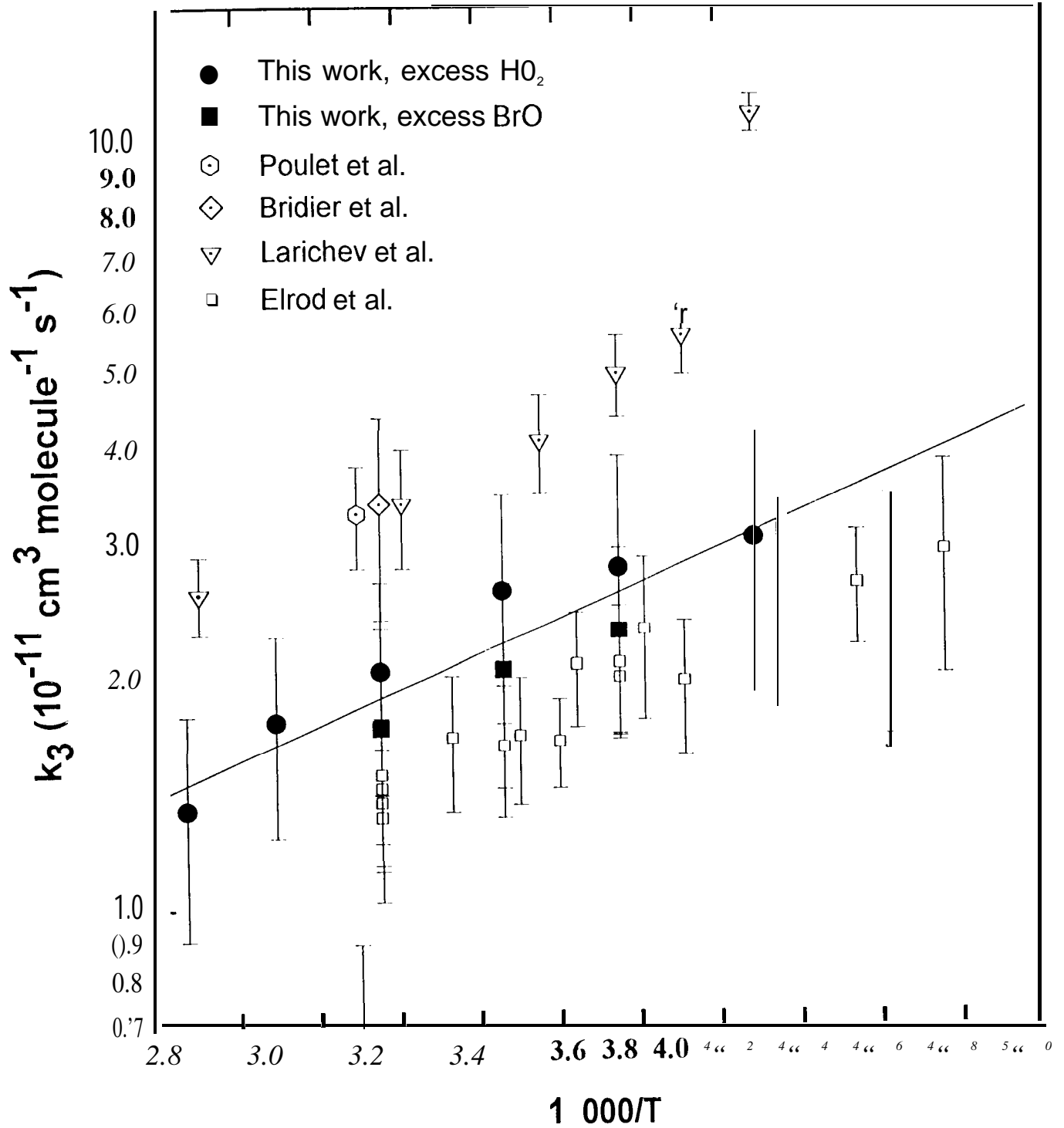


Figure 9